

Provided for non-commercial research and education use.
Not for reproduction, distribution or commercial use.



This article appeared in a journal published by Elsevier. The attached copy is furnished to the author for internal non-commercial research and education use, including for instruction at the authors institution and sharing with colleagues.

Other uses, including reproduction and distribution, or selling or licensing copies, or posting to personal, institutional or third party websites are prohibited.

In most cases authors are permitted to post their version of the article (e.g. in Word or Tex form) to their personal website or institutional repository. Authors requiring further information regarding Elsevier's archiving and manuscript policies are encouraged to visit:

<http://www.elsevier.com/copyright>



Theoretical study of the adsorption of rhodium on a $\text{TiO}_2(1\ 1\ 0)\text{-}1 \times 1$ surface

P. Mutombo^{a,*}, N. Balázs^b, Z. Majzik^{a,b}, A. Berkó^b, V. Cháb^a

^a Institute of Physics of Academy of Sciences of the Czech Republic, Cukrovarnická 10, 16253 Praha 6, Czech Republic

^b Reaction Kinetics Laboratory, Institute of Nanochemistry and Catalysis, CRC of the Hungarian Academy of Sciences, University of Szeged, P.O. Box 168, H-6701 Szeged, Hungary

ARTICLE INFO

Article history:

Received 8 December 2011

Received in revised form

22 December 2011

Accepted 1 January 2012

Available online 24 January 2012

Keywords:

Density functional theory

Rhodium

Oxide surface

Scanning tunneling spectroscopy

ABSTRACT

Density functional theory (DFT) calculations were used to study the adsorption of rhodium on a $\text{TiO}_2(1\ 1\ 0)\text{-}1 \times 1$ surface as a function of coverage. It was found that Rh atom prefers the hollow site between a bridging oxygen atom, a threefold oxygen atom and a fivefold coordinated Ti atom, regardless of the coverage used. DFT calculations also suggest that Rh–Rh interaction is attractive along the $[0\ 0\ 1]$ direction, implying that the Rh 1D nanostructure should grow preferentially along this direction. Simulated Rh dimer clusters resemble strongly Pd dimers resolved in STM experiments suggesting that both metals occupy the same adsorption site at the $\text{TiO}_2(1\ 1\ 0)$ surface.

© 2012 Elsevier B.V. All rights reserved.

1. Introduction

Great advances were achieved recently in the investigation of the interaction between metals and oxide surfaces. Metal thin films were prepared on these surfaces in a well-defined manner with respect to the dimension, shape, particle size and electronic structure. The chemisorption of metals on these surfaces as well as the catalytic reactions are linked to the particle size, their thickness and the nature of the oxide support [1–3].

One of the most used metals in heterogeneous catalysis is rhodium. Like Pt, Rh is used in converters in automobiles for the transformation of harmful pollutants from the exhaust system. Rhodium particles finely dispersed, supported on metal oxides influence catalytically reactions such as the hydrogenation [4] and oxidation of carbon monoxide [5,6], reduction of nitrogen oxide [7] and the hydroformylation of olefins [8]. Using a method so-called “sewing and growing”, Berko et al. could produce two kinds of Rh nanoparticles on a reconstructed $\text{TiO}_2(1\ 1\ 0)$ surface. They obtained particles of hexagonal shape and 1D elongated nanoparticles oriented in the $[0\ 0\ 1]$ direction [9]. Note that the Rh 1D elongated particles have been grown on both the (1×1) and (1×2) reconstructed surfaces by increasing the surface temperature during the growth process [10]. STM measurements of the same system at low coverage show small Rh clusters located on top of the reduced Ti_xO_y stripes [10]. Moreover, according to experimental findings platinum group metals such that Pd and Pt prefer to adsorb on top

of the Ti_5 rows at the $\text{TiO}_2(1\ 1\ 0)$ surface [3,11,12]. Since Rh belongs to the same group and share with them similar chemical properties, one expects that it will exhibit similar behavior.

Density functional theory (DFT) calculations [13] performed to determine the adsorption geometry of Pd on the $\text{TiO}_2(1\ 1\ 0)$ surface, indicate that Pd can sit stably either above the two-fold coordinated oxygen or above the Ti rows. However, another theoretical work shows, that Pd prefers adsorption sites along the surface channels near to the fivefold-coordinated Ti atoms but tilted toward the O_{2c} atoms [14]. The latter adsorption geometry was also suggested when a single Pt atom was placed at the stoichiometric $\text{TiO}_2(1\ 1\ 0)$ surface [15,16].

All three metals form 1D metallic structures on $\text{TiO}_2(1\ 1\ 0)$ surface [3,9–11]. These 1D nanowires tend to grow along the $[0\ 0\ 1]$ direction. Since $\text{TiO}_2(1\ 1\ 0)$ is a wide band gap material, such nanostructures can be electrically isolated from any other substrate by the support. This constitutes a huge potential in nanoscale electronics. The growth of 1D particles has been ascribed to anisotropic surface diffusion of metal adatoms during the nucleation process [17,18], anisotropic distribution of bonding sites (defects for example) of different strength around the perimeter of the particles [2,19] or to variation of interface energy affected by a lattice mismatch of the lowest-energy plane of the material that forms the particle [3,20].

We aim to perform total energy DFT calculations to determine the adsorption geometry of a single Rh atom at a $\text{TiO}_2(1\ 1\ 0)$ surface at different coverages. To the best of our knowledge, such calculations have not been carried out before. These calculations will enable us to explain the preferential alignment of the 1D nanostructure along the $[0\ 0\ 1]$.

* Corresponding author. Tel.: +420 220 318 503; fax: +420 233 343 184.
E-mail address: mutombo@fzu.cz (P. Mutombo).

2. Methods

2.1. Computational techniques

We performed DFT calculations within the local density approximation (LDA) [21]. We use ultrasoft Vanderbilt pseudopotentials [22] and plane waves with a cutoff energy of 30 Ry. The charge density cutoff energy was set to 300 Ry. The Ti pseudopotential has a $3s^2 3p^6 4s^2 3d^1$ configuration including the 3s, 3p semicore states. The oxygen and the Rh atoms were described by a $2s^2 p^4$ and a $4d^8 5s^1$ electron configuration respectively. A 15 Å thick vacuum region was used to prevent spurious interaction between the image slabs. To model the clean $\text{TiO}_2(110)-1 \times 1$ surface, we used a slab made of 9 atomic layers (three TiO_2 layers). Different unit cells were employed, namely 3×2 , 3×1 and 1×1 corresponding to 1/6ML, 1/3ML and 1ML coverage respectively. Note that the coverage is determined according to the number of bridging oxygen atoms per unit cell. The distance between two Rh atoms in [001] direction was 8.76 Å and 2.92 Å for the 3×2 (3×1) and 1×1 supercell respectively. A single Rh atom was placed at both sides of the slab, at the following adsorption sites (Fig. 1): on top of a bridging oxygen atom (T_1), bridging the two topmost oxygen atoms (Br_1), at the fourfold hollow site between the bridging oxygen atom, the threefold oxygen atom and the fivefold coordinated Ti atom (H_2), on top of a fivefold coordinated Ti atom (T_5) and, finally at the fourfold hollow site over the fivefold coordinated Ti atom (H_1). The initial position of Rh in the starting geometry was chosen taking into account the sum of covalent radii between Rh and involved atoms (bridging oxygen and fivefold coordinated Ti atoms). All atoms of the slabs, except the inner TiO_2 layer, were allowed to relax until the Hellman–Feynman forces were within 10 meV/a.u. The Quantum-ESPRESSO package was used for all calculations [23]. The integration in the Brillouin zone was done using a $4 \times 4 \times 1$ Monkhorst-Pack grid for the 1×1 unit cell. Correspondingly reduced k-point grids were used for bigger unit cells.

To find out the direction of preferential growing of the 1D particles, we needed to determine the direction of the strongest Rh–Rh interaction. We considered two models: in the first model, the 1D atomic chain consists of Rh atoms sitting at their best adsorption site; in the second, the 1D atomic chain is made of Rh atoms occupying the oxygen vacancies. For this purpose, we used a 2×2 unit cell in which two Rh atoms were put at their best adsorption sites or at the oxygen defects to simulate growing of an infinite atomic chain in the [001] or [011] directions. Several configurations were considered (Figs. 2 and 3). The configuration

Table 1

Total energy differences dE (eV) of different configurations with respect to the energy of best adsorption site at different coverages.

Configurations	dE (eV)	dE (eV)	dE (eV)
	1/6ML	1/3ML	1ML
H_1	0.37	0.45	0.91
H_2	0	0	0
Br	0.12	0.37	1.53
T_1	3.15	3.42	1.64
T_5	2.88	2.95	2.62

with the lowest total energy indicated the direction of preferential growth.

3. Results and discussions

Fig. 1 displays top and side views of the $\text{TiO}_2(110)-1 \times 1$ surface including the adsorption sites used in the calculations. To determine the best adsorption site of rhodium on a clean $\text{TiO}_2(110)$, we used a stoichiometric 1×1 Rh-covered surface. Total energy calculations indicated that a single Rh atom would prefer a fourfold hollow site between a bridging oxygen atom, a threefold oxygen atom and a fivefold coordinated Ti atom, the so-called H_2 position (Table 1). This position was also the best one for all other investigated coverages. Similar adsorption site was found also for isolated Pd and Pt atoms on the same surface [14–16]. Rh lies 0.5 Å above the atomic plane of the O_{2c} atoms. Rh was bonded to a bridging oxygen and a Ti_5c cation by bond lengths of 2.02 and 2.23 Å respectively. The bond length to oxygen corresponds approximately to the sum of covalent radii (1.98 Å), while the bonding distance to Ti atom is contracted, indicating a strong Rh–Ti bond. The adsorption of Rh at the H_2 position induced a distortion of surrounding atoms. The O_{2c} atoms moved up by 0.04 Å in average while the Ti_{6c} atoms shifted down by 0.05 Å. The Ti_{5c} bonded to the Rh bond relaxed up by 0.12 Å while the other Ti_{5c} cations were almost unaffected. The O_{3c} nearer Rh moved up by 0.10 Å in contrast to those far away which slightly relaxed down by 0.03 Å in average.

All these relaxations refer to the atomic positions in the clean relaxed $\text{TiO}_2(110)$ [24]. The second best position was found to be the Br site for smaller coverages (1/6ML and 1/3ML). At 1ML, the H_1 becomes the second best adsorption site. This is due to the reorganization of the Rh atoms at the surface connected to the higher coverage.

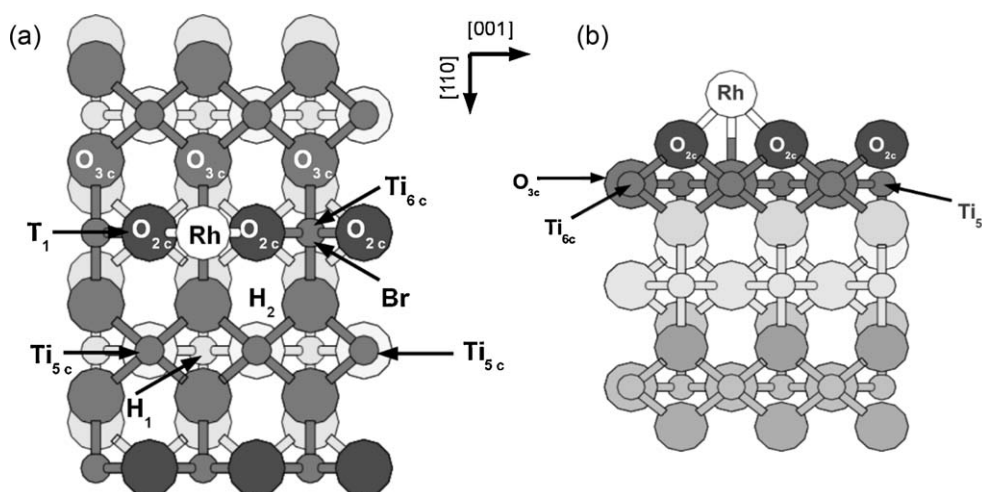


Fig. 1. Top (a) and side (b) views of the $\text{Rh}/\text{TiO}_2(110)-1 \times 1$ system. The different kind of atoms and adsorption sites are indicated. Rh atom in the “Br” position is shown.

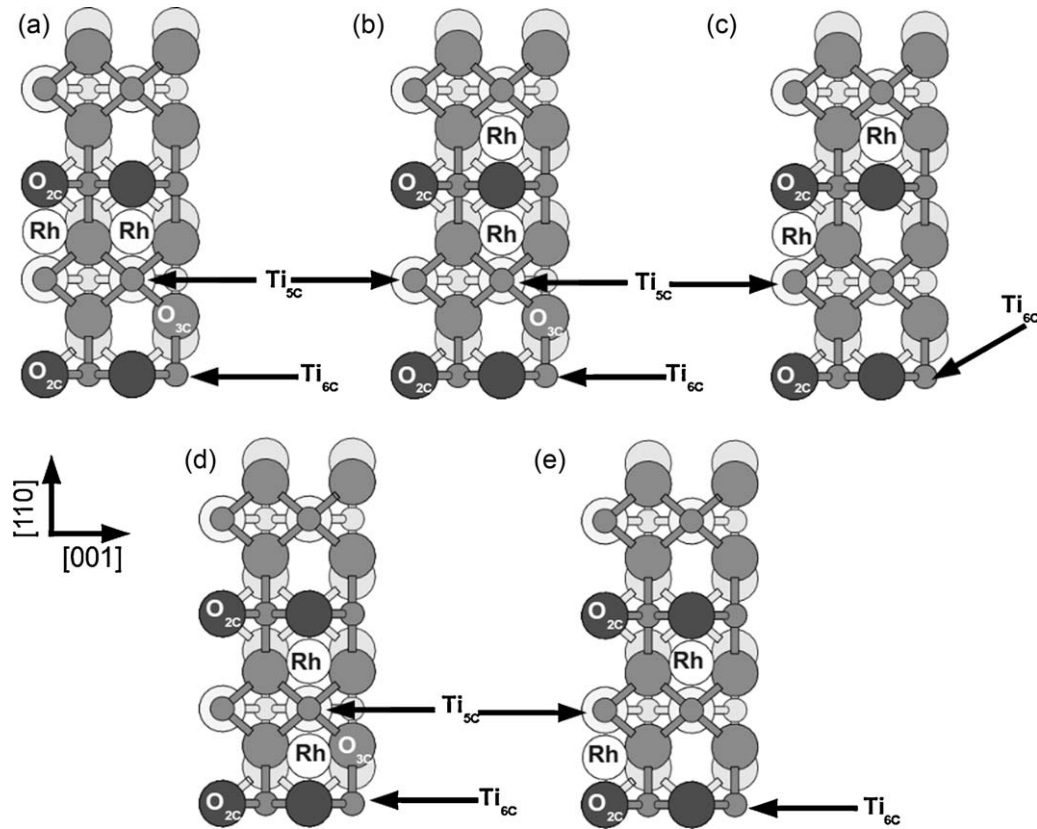


Fig. 2. Model "1": Test configurations for determining the strongest Rh–Rh interaction. Rh atoms were placed at their best adsorption site.

4. Preferential growth of Rh 1D nanostructure along the (001) direction

In order to explain the 1D Rh preferential growing according to model "1", two Rh were placed at the H₂ sites as displayed in Fig. 2. It is worth noting that the Rh atoms will interact

differently depending on the distance between them. The interplay between adsorbate–adsorbate interaction on the one hand and adsorbate–substrate interaction on the other, is determinant for further growth of the 1D Rh structure. Comparison between all structures based on model "1" (see Fig. 2) suggests that the structure "a" with the Rh atoms aligned along the [001] direction has

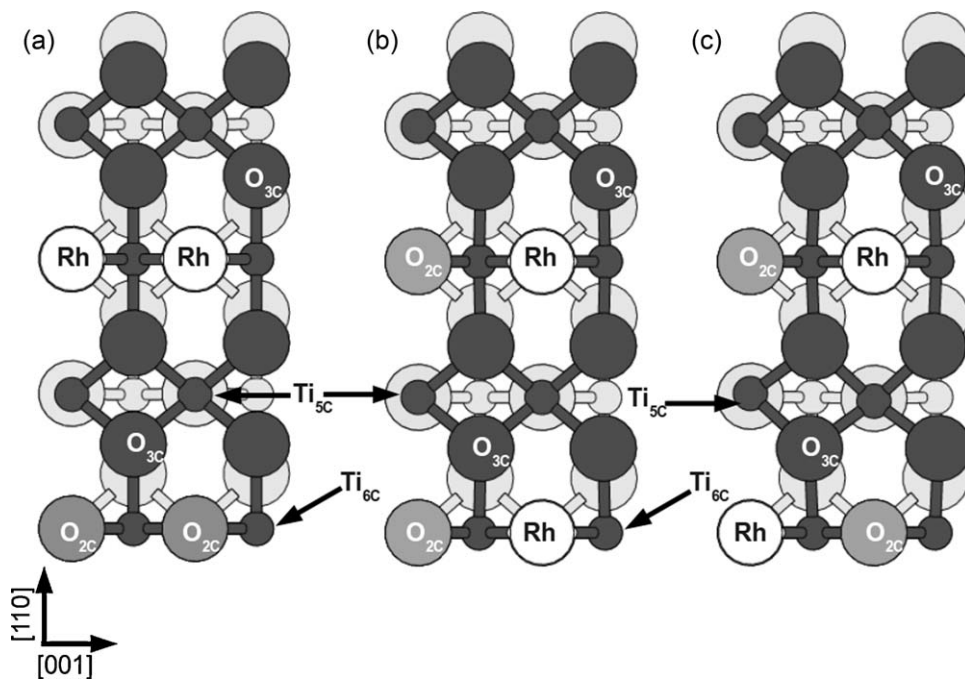


Fig. 3. Model "2": Test configurations for determining the strongest Rh–Rh interaction: Rh atoms were placed at the bridging oxygen vacancies.

Table 2

Total energy differences dE (eV) of different configurations of models “1” and “2” with respect to the energy of the best adsorption site in each model.

Configurations	dE (eV)	Initial distance between Rh atoms (Å)
Model 1		
a	0	2.92
b	5.44	3.21
c	2.72	4.34
d	0.27	3.21
e	1.90	4.34
Model 2		
a	0	2.92
b	2.85	6.42
c	2.72	7.05

the lowest energy (Table 2). The next lowest energy configuration “d” is higher by 0.27 eV. Note that in the latter structure, both Rh atoms were placed at a same distance as in the configuration “b”. However, the “b” structure has the highest energy. The difference between these two structures consists in the fact that in “b”, Rh atoms interact across the bridging oxygen rows while they do not in configuration “d”. One may conclude that the bridging oxygen row constitutes some kind of a barrier to the Rh–Rh interaction.

Growth of Rh particles in the $[1\ 1\ 0]$ direction will be consequently impeded. Similar situation is also observed if we compare configurations “c” and “e”. In “c”, Rh atoms interact across the oxygen rows. This gives rise to higher total energy compared to structure “e”.

The configuration “a” in which the Rh atoms are oriented along the $[0\ 0\ 1]$ was also found favorable for structures based on model “2”. In this model, Rh atoms were placed at the oxygen vacancies. This leads to the upward relaxation of the nearby bridging oxygen atoms by 0.05 Å. The Ti_{6c} atoms bonded to them moved down by 0.09 Å. The Rh– Ti_{6c} distance was found to be 2.32 Å. On the other hand, the Ti_{5c} cations relaxed up by 0.04 Å. All these changes are related to the atomic positions in the clean relaxed $TiO_2(1\ 1\ 0)$ slab [24]. Note that Rh atoms were higher by 0.64 Å with respect to the neighboring bridging oxygen atoms.

These findings suggest that the distance between the Rh atoms as well as the presence of oxygen atoms running perpendicular to the growth direction is crucial for determining the best configuration. It is apparent that the longer the distance the weaker the interaction between the Rh atoms. The Rh–Rh interaction in the Rh/ $TiO_2(1\ 1\ 0)$ system is attractive. Removal of oxygen atoms should ease the growing of Rh atomic chains along the $(1\ 1\ 0)$ direction.

5. STM simulations

We simulated STM images of a Rh atom sitting in a H_2 position (at a coverage of 1/6ML) and of Rh small clusters made according to the two models mentioned above, i.e. by placing two (dimer) or three (trimer) Rh atoms at the H_2 site and an oxygen vacancy respectively. We used a 6×2 unit cell to minimize the interactions between the clusters and their periodic image. We wanted to compare simulated Rh clusters to Pd ones obtained at the $TiO_2(1\ 1\ 0)-1 \times 1$ surface [11]. Pd clusters look as sitting on-top on the Ti_5 rows. There is no experimental evidence of Pd trimers. All STM simulations were done according to the Tersoff–Hamann approximation [25] at 1.7 V, in a constant-height mode (z : constant). Fig. 4 displays a STM map of a single Rh atom at the surface. Rh appears as a bright protrusion located on-top of a Ti_5 row suggesting a strong mixing between Rh and Ti electronic states.

Also, simulated Rh dimer and trimer clusters made according to model “1” appear as sitting on the Ti rows (Figs. 5 and 6). The

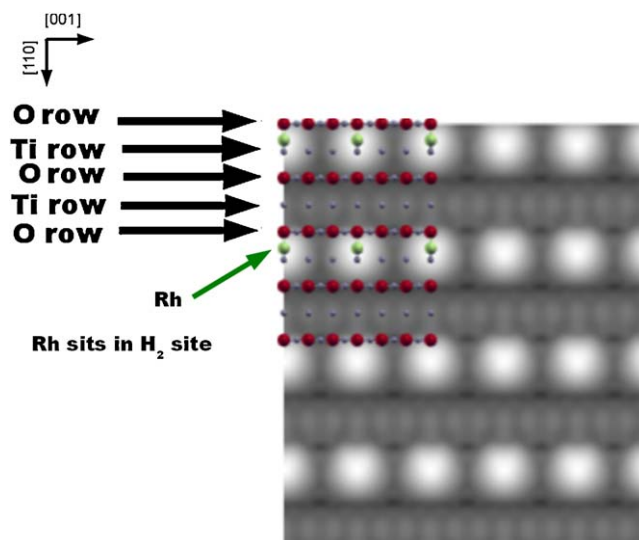


Fig. 4. Simulated STM of a Rh atom at a coverage of 1/6ML. Bias voltage: 1.7 V, $z=3$ Å.

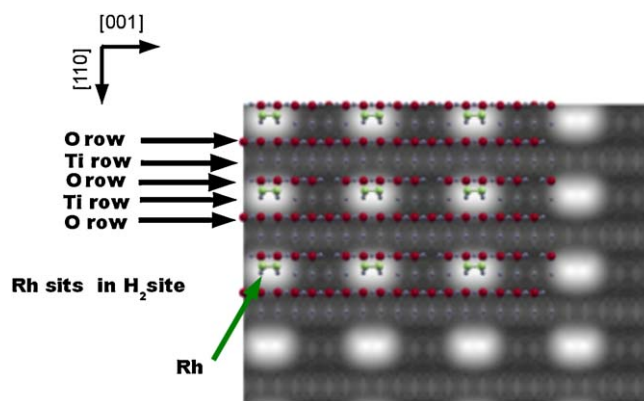


Fig. 5. Simulated STM of a Rh dimer made according to model “1”. Bias voltage: 1.7 V, $z=5$ Å.

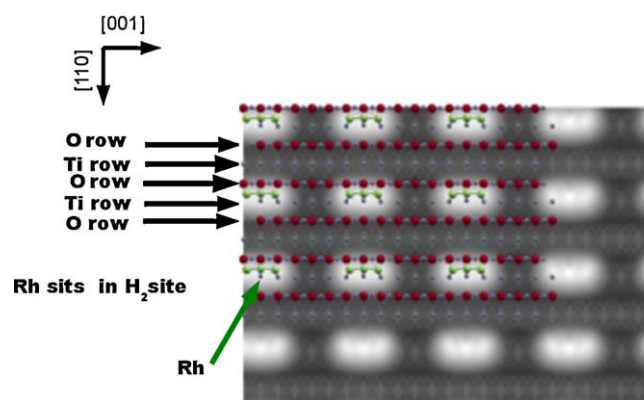


Fig. 6. Simulated STM of a Rh trimer made according to model “1”. Bias voltage: 1.7 V, $z=5$ Å.

Rh dimer resembles strongly to the Pd clusters [11]. The trimer looks asymmetric due its distorted structure (one-up-two-down configuration). The vertical separation between the up and down atoms was 0.2 Å. The calculated Rh–Rh bond length in the clusters was 2.46 Å.

Figs. 7 and 8 display simulated dimer and trimer made according to model “2”. Both types of clusters appear located on the O rows. Since such clusters have not been observed in any STM

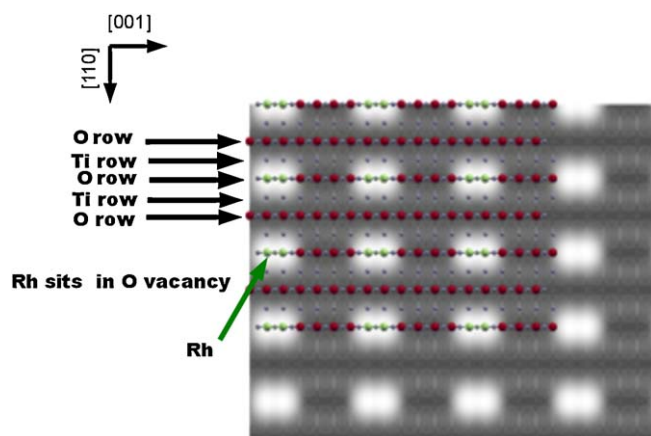


Fig. 7. Simulated STM of a Rh dimer made according to model "2". Bias voltage: 1.7 V, $z=5 \text{ \AA}$.

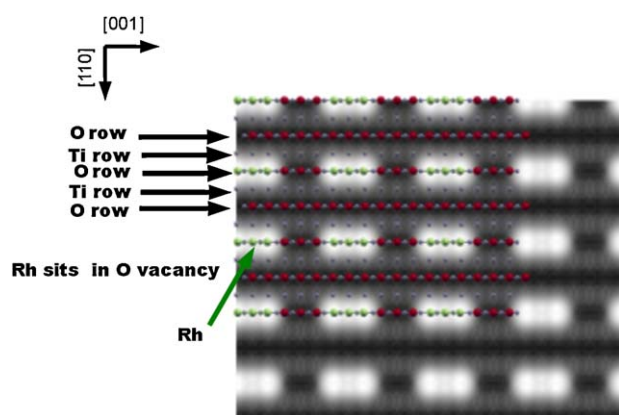


Fig. 8. Simulated STM of a Rh trimer made according to model "2". Bias voltage: 1.7 V, $z=5 \text{ \AA}$.

measurements, we may conclude that experimental Rh clusters are likely made of Rh sitting at the fourfold hollow site between the bridging oxygen and the Ti rows.

6. Conclusions

We studied the adsorption behavior of Rh on the $\text{TiO}_2(110)$ surface using DFT total energy calculations. We have found that a Rh

atom prefers the fourfold hollow site (H_2) between the bridging oxygen row and the Ti cations. Total energy calculations also suggest that rhodium particles should grow preferentially along the $[001]$ direction in agreement with experimental findings. Simulated STM images of a Rh atom and Rh clusters sitting in the H_2 site appear as bright features located on-top of Ti_5 rows.

Acknowledgment

This work was supported by the Czech-Hungarian Intergovernmental Science&Technology Program (CZ-06/2008 TÉT).

References

- [1] C.T. Campbell, Surf. Sci. Rep. 27 (1–3) (1997) 1.
- [2] K. Katsiev, M. Batzill, U. Diebold, Phys. Rev. Lett. 98 (2007) 186102.
- [3] D.S. Humphrey, G. Cabailh, C.L. Pang, C.A. Muryn, S.A. Cavill, H. Marchetto, A. Potenza, S.S. Dhesi, G. Thornton, Nanoletters 9 (1) (2009) 155.
- [4] J.-C. Tsai, M.N. Kenneth, J. Am. Chem. Soc. 114 (13) (1992) 5117.
- [5] T. Ioannides, A.M. Efstathiou, Z.L. Zhang, X.E. Verykios, J. Catal. 156 (1995) 265.
- [6] S. Fuchs, T. Hahn, H.-G. Lintz, Chem. Eng. Process. 33 (1994) 363.
- [7] B.E. Hayden, A. King, M.A. Newton, N. Yoshikawa, J. Mol. Catal. A: Chem. 167 (2001) 33.
- [8] S.S.C. Chuang, S.I. Pien, J. Catal. 135 (1992) 618.
- [9] A. Berko, J. Szökő, F. Solymosi, Solid State Ionics 141–142 (2001) 197.
- [10] Z. Majzik, N. Balázs, A. Berkó, J. Phys. Chem. C 115 (2011) 9535.
- [11] C. Xu, X. Lai, G.W. Zajac, D.W. Goodman, Phys. Rev. B 56 (1997) 13464.
- [12] A. Berkó, J. Szökő, F. Solymosi, Surf. Sci. 532–535 (2003) 390.
- [13] T. Bredow, G. Pacchioni, Surf. Sci. 426 (1999) 106.
- [14] J.F. Sanz, A. Marquez, J. Phys. Chem. C 111 (2007) 3949.
- [15] V. Çelik, H. Ünal, E. Mete, Ş. Ellialtıoğ lu, Phys. Rev. B 82 (2010) 205113.
- [16] H. Iddir, S. Ögüt, N.D. Browning, M.M. Disko, Phys. Rev. B 72 (2005) 081407(R).
- [17] F.J. Himpsel, J.L. McChesney, J.N. Crain, A. Kirakosian, V. Pérez-Dieste, N.L. Abbott, Y.-Y. Luk, P.F. Nealey, D.Y. Petrovykh, J. Phys. Chem. B 108 (2004) 14484.
- [18] M.J.J. Jak, C. Konstapel, A. van Kreuningen, J. Verhoeven, J.W.M. Frenken, Surf. Sci. 457 (2000) 295.
- [19] W.T. Wallace, B.K. Min, D.W. Goodman, Top. Catal. 34 (2005) 17.
- [20] J. Kibsgaard, B.S. Clausen, H. Topsøe, E. Lægsgaard, J.V. Lauritsen, F. Besenbacher, J. Catal. 263 (2008) 98.
- [21] J. Perdew, A. Zunger, Phys. Rev. B 23 (1981) 5048.
- [22] D. Vanderbilt, Phys. Rev. B 41 (1990) 7892.
- [23] P. Giannozzi, S. Baroni, N. Bonini, M. Calandra, R. Car, C. Cavazzoni, D. Ceresoli, G.L. Chiarotti, M. Cococcioni, I. Dabo, A. Dal Corso, S. De Gironcoli, S. Fabris, G. Fratesi, U.G.R. Gebauer, C. Gougoussis, A. Kokalj, M. Lazzeri, L. Martin-Samos, N. Marzari, F. Mauri, R. Mazzarello, S. Paolini, A. Pasquarello, L. Paulatto, C. Sbraccia, S. Scandolo, G. Sclauzero, A.P. Seitsonen, A. Smogunov, P. Umari, R.M. Wentzcovitch, J. Phys.: Condens. Matter 21 (2009) 395502.
- [24] P. Mutombo, A.M. Kiss, A. Berkó, V. Cháb, Nanotechnology 17 (2006) 4112.
- [25] J. Tersoff, D.R. Hamann, Phys. Rev. Lett. 50 (1983) 1998; J. Tersoff, D.R. Hamann, Phys. Rev. B 31 (1985) 805.